

## 7.7 Advances in Building Energy Research

### **Thermal and sound insulation performance assessment of vacuum insulated composite insulation panels for building façades**

Fin O’Flaherty<sup>a\*</sup>, Mahmood Alam<sup>b</sup>

*<sup>a</sup>Materials and Engineering Research Institute, Sheffield Hallam University, Howard Street,  
Sheffield, UK, S1 1WB*

*<sup>b</sup>School of Environment and Technology, University of Brighton, Moulsecoomb Campus,  
Lewes Road, Brighton, UK, BN2 4GJ*

**\*Corresponding author email: [f.j.oflaherty@shu.ac.uk](mailto:f.j.oflaherty@shu.ac.uk)**

**Telephone: 00 44 (0)114 225 3178**

**Orcid IDs:** <sup>a</sup>0000-0003-3121-0492; <sup>b</sup> 0000-0001-9395-6252

# **Thermal and sound insulation performance assessment of vacuum insulated composite insulation panels for building façades**

## **Abstract**

Composite insulation panels (CIPs) currently used in building façades require significant design changes e.g. increased thickness to realise higher thermal and sound insulation performance. This study deals with the manufacturing and characterisation of smart façade panels for achieving higher thermal and sound insulation dual characteristics in one panel without a significant increase in thickness. Prototype panels were manufactured using vacuum insulation core (VIC) combined with mass loaded vinyl (MLV) layers. Thermal transmission and weighted sound reduction index ( $R_w$ ) was experimentally measured in the laboratory. The results were compared with a control panel made with extruded polystyrene (XPS) core. The VIC panel showed a 51% improvement in the centre of panel U-value compared to control XPS core panel of the same thickness. Integrating the two MLV layers inside of aluminium skins either side of the vacuum insulation panel led to 3dB improvement in  $R_w$  from 32 dB to 35 dB which could be further improved by optimising the MLV layer positioning in the CIP and better bonding between the MLV and the vacuum insulation panel. This shows that vacuum insulation core panels combined with MLV offers a solution to achieve smart building façade with excellent thermal and sound insulation performance.

**Keywords:** Building façade; Thermal insulation; Sound insulation, Vacuum insulation panel; Mass Loaded Vinyl

## List of Symbols

$A$	Area [ $\text{m}^2$ ]
$A_e$	Equivalent absorption area of the receiver room [ $\text{m}^2$ ]
$d$	Thickness of the sample [m]
$d_c$	thickness of core material [m]
$\Delta T$	Temperature difference between hot and cold surfaces of sample [K]
$f$	Frequency [Hz]
$K_R$	Constant value 42.3 for normal incidence and 47.3 for random angle of incidence
$L_r$	Average sound pressure level in the Receiver room [dB]
$L_s$	Average sound pressure level in the Source room [dB]
$m$	Mass [kg]
$q_x$	Heat flux in direction $x$ [ $\text{Wm}^{-2}$ ]
$R$	Sound reduction index [dB]
$R_{si}$	Internal surface resistance [ $\text{m}^2\text{KW}^{-1}$ ]
$R_{se}$	External surface resistance [ $\text{m}^2\text{KW}^{-1}$ ]
$R_w$	Weighted sound reduction index [dB]
$S$	Surface area of common partition or panel [ $\text{m}^2$ ]
$T$	Temperature [K]
$t$	Reverberation time [s]
$t_i$	thickness of internal facing [m]
$t_e$	thickness of external facing [m]
$U$	Thermal transmittance [ $\text{Wm}^{-2}\text{K}^{-1}$ ]
$V$	Volume of the receiving room [ $\text{m}^3$ ]
$\lambda$	Thermal conductivity [ $\text{Wm}^{-1}\text{K}^{-1}$ ]
$\lambda_c$	Thermal conductivity of core material [ $\text{Wm}^{-1}\text{K}^{-1}$ ]
$\lambda_{fe}$	Thermal conductivity of external facing layer [ $\text{Wm}^{-1}\text{K}^{-1}$ ]
$\lambda_{fi}$	Thermal conductivity of internal facing layer [ $\text{Wm}^{-1}\text{K}^{-1}$ ]

## 1. Introduction

Energy efficiency in buildings is one of the most significant factors to reduce their impact on the environment. Energy consumption in buildings contribute considerably to the carbon emissions. In the EU, buildings consume 40% of energy and are responsible for 36% of CO<sub>2</sub> emissions (EU Commission, 2017). Insulating the building envelope is key to achieving savings on building space heat energy and reducing carbon emissions. Today's buildings require envelopes with high thermal insulation performance while also achieving excellent sound insulation. Choice of materials for use in building envelopes is an important consideration for meeting the thermal and sound insulation requirements. In modern buildings facades, Composite Insulation Panels (CIP), also known as sandwich panels, are increasingly being used due to their thermal and sound insulation properties, lightweight, aesthetics and ease of production and installation (Davies, 2001; Alam & O'Flaherty, 2016). CIPs are generally made by bonding polymeric foam, mineral fibre, or honeycomb cores with metallic or non-metallic outer facings. Currently, CIPs made with lightweight core material, for instance low density foam or fibres bonded between two outer skins are more commonly applied in building façades. Thermal insulation performance of these panels is measured by their thermal transmission value i.e.  $U$ -value. Lower  $U$ -values represent higher thermal insulation performance of CIPs. Presently, the  $U$ -value of CIPs can be reduced by increasing the thickness of the thermal insulation core material. However, this approach may not be suitable for achieving smart building envelope design and may not be technically feasible in some buildings. This requires that alternative high thermal performance core materials need to be employed in order to improve energy conservation in the building without having any impact on thickness of the CIP. Also, for any building element, sound insulation properties need to be considered along with their thermal insulation properties.

Sound insulation performance of foam core CIPs is often insufficient (Ballagh, 2010) and regularly, an extra sound barrier layer is needed. Sound insulation of CIPs is measured by evaluating the Sound Reduction Index ( $R$ ) which is a frequency dependent parameter. Generally, sound reduction index of foam core panels is around 30 dB (Ballagh, 2010). Mostly, mineral wool is used where higher sound insulation is required (Azimi, 2017) but has lower thermal insulation and compressive strength properties. The sound transmission loss of a building element can be increased by adding mass to the element according to the Mass Law which states that sound insulation increases by almost 6 dB for every doubling of mass or frequency provided that the panel behaves as a single solid component (Praščević, Cvetković, Mihajlov, 2012). Mass Law can be described mathematically as shown in Equation 1 (Long, 2014; Tadeu & Mateus, 2001)

$$R = 20 \log(f \times m) - K_R \quad (1)$$

$K_R$  is a constant which is 42.3 for normal incidence and 47.3 for random angle of incidence.

Additional sound barrier layers can be used to increase the sound transmission resistance of lightweight panels (Wareing, Davy, Pearse, 2015). However, any additional layer for sound insulation performance adds thickness and weight to the overall panel which may lead to design complexities and installation difficulties. This additional sound insulation layer may also lead to a reduction in the core thermal insulation thickness with the consequences of reducing thermal performance and increasing weight of the panel. Ideally, the improved sound insulation properties of CIPs need to be achieved with minimal effect on the thickness, thermal performance and weight of the panel.

Within this context, this paper looks at developing and characterising CIPs made with vacuum insulation core and investigating the effect on thermal and sound insulation performance.

## **2. Research Significance**

Vacuum insulation has been reported as an energy efficient alternative thermal insulation to conventional building insulation materials (Brunner & Simmler, 2008; Baetens et al., 2010; Alam, Singh & Limbachiya, 2011, Alam, Singh, Suresh & Redpath, 2017). The advantage of vacuum insulation over conventional thermal insulation materials (e.g. extruded polystyrene foam, XPS) is that it can improve the thermal resistance of the building element without increasing the thickness owing to its low thermal conductivity of  $0.004 \text{ Wm}^{-1}\text{K}^{-1}$  (centre of panel) and  $0.007 \text{ Wm}^{-1}\text{K}^{-1}$  (including edge effects and ageing) (Wakili, Bundi & Binder, 2004). Use of vacuum insulation in buildings as a component in thermal composite insulation systems along with other insulation materials for achieving higher thermal resistance has been researched in number of studies (Hayez & Kragh, 2013; Mandilaras, Atsonios, Zannis, Founti, 2014; Voellinger, Bassi, Heitel, 2014; Kan and Hu 2017). Biswas et al., (2018) researched the use of vacuum insulation in composite insulation boards and found that vacuum insulation improved the thermal resistance by approximately two times compared to currently used insulation in buildings. However, these studies have only focused on the thermal insulation aspects. Only a few studies (Cauberg & Tenpierik, 2007; Maysenhölder, 2008, Walters & Dance, 2014) have looked at the effect of vacuum insulation cores (VIC) on the sound insulation properties. Walters & Dance, 2014 have tried to establish the relationship between the sound insulation potential and degree of vacuum in vacuum insulation panels. Cauberg & Tenpierik (2007) employed 20 mm vacuum insulation core between 3 mm TRESPA facings and the weighted sound reduction index measured was 27 dB. Maysenhölder (2008) tested 11mm thick vacuum insulation core sandwiched between rubber and aluminium facings and measured values of weighted sound reduction index were found to be 32 dB and 29 dB for

glued and non-glued samples respectively. This shows that weighted sound reduction of VIC sandwich elements is more or less comparable to the foam core counterparts. Hence, any building panels containing VIC will require additional acoustic treatment to improve its sound insulation properties. However, it is crucial that the VIC remains intact i.e. it does not get punctured during manufacture or installation for utilisation of its key property. This paper describes the development and characterisation of CIPs made of vacuum insulation core and investigates their thermal insulation performance with consideration given to protecting the VIC from damage. Additionally, the effect of adding sound barrier layers on the sound insulation performance of the investigated panels with vacuum insulated and extruded polystyrene (XPS) cores has also been investigated to enable its design to be optimised for thermal, sound and weight without duly affecting the overall thickness.

### **3. Preparation of composite insulation panel (CIP) samples**

A number of composite insulation panels were manufactured with the aim of testing them in the laboratory to determine thermal and acoustic properties. This will lead to optimum performance through a design approach to minimise thickness and enhance durability. Two different CIPs were designed and manufactured for the thermal investigation (Section 3.1) whereas five panels were manufactured for the acoustic investigation (Section 3.2).

#### ***3.1 CIPs for thermal insulation investigation***

The investigated CIP samples were manufactured by sandwiching vacuum insulation and extruded polystyrene (XPS) layers as core material between two outer aluminium facing layers at Panel Systems Ltd., Sheffield, UK (Table 1). For this purpose commercially available vacuum insulation and XPS samples were obtained from relevant suppliers. CIP prototype for thermal investigation consisted of the following layers of materials: aluminium, XPS, vacuum

insulation, XPS, aluminium and the manufacturing process is shown in Figure 1. An XPS edge border was placed around the VIP and XPS layers, the main purpose being to protect vacuum insulation from any physical damage at the edges of the panel where it would be exposed to puncturing. In this study, width of the XPS edge was 95 mm (width side) and 97.5 mm (length side) so that overall size of the panel fits the size requirements of the thermal transmission testing chamber. Ideally, the XPS edge border should be smaller e.g. 25 mm so that the panel comprises a high proportion of vacuum insulation (the influence of border area to panel area is considered in Section 5.3). None of the vacuum insulation was visible once the aluminium facings were bonded thereby reducing the risk of accidental damage during handling and installation. Thermal conductivities of VIC and XPS samples were also determined before use. The control CIP (Panel T1) was manufactured with only 25mm thick XPS as the core material whereas the vacuum insulated panel (T2) consisted of 20mm thick vacuum insulation and XPS (2x3mm) core material. The vacuum insulated area in the VIC panel was 600 mm x 300 mm comprising two vacuum insulation cores side-by-side each with the dimensions 300 mm x 300 mm. The overall size of both CIP samples was the same (790mm x 495mm).

**[Table 1 near here]**

**[Figure 1 near here]**

### ***3.2 CIPs for sound insulation investigation***

Multi-layered CIPs were manufactured with the aim of optimising sound as well as thermal insulation characteristics. The CIPs were prepared in a sandwich-type structure made up of a mass loaded vinyl (MLV) layer bonded between a core of XPS and vacuum insulation and aluminium facings. The purpose of the additional MLV layer was to provide sound insulation while retaining excellent thermal insulation. An MLV layer adds weight to the CIP and provides a vibration dampening function for aluminium facings while the XPS and vacuum insulated

core provides thermal insulation. Composition, weight and thickness of the CIP prototypes are given in Table 2. Referring to Table 2, the CIP prototypes No. A2 (AMXA), No. A3 (AMXMA) and No. A5 (AMVMA) were manufactured to evaluate the sound insulation differences produced by the addition of the MLV layers and compared with the MLV-free control CIPs No. A1 (AXA) and No. A4 (AXVXA). All CIP prototypes were manufactured to the size of 566 mm × 566 mm to fit the opening of the acoustic chamber. Layout of different layers for Panels A1 to A4 is shown in Figure 2. Panel A5 is omitted from Figure 2 but is similar in composition to Panel A4 except that both 3mm thick XPS layers were replaced with 2.5 mm thick MLV layers. The manufacturing process of one panel from Table 2 (Panel A4) is shown in Figure 3.

**[Table 2 near here]**

**[Figure 2 near here]**

**[Figure 3 near here]**

## **4 Thermal and sound insulation measurement**

### ***4.1 Thermal conductivity measurement of vacuum insulation panel***

Thermal conductivity ( $\lambda$ ) in one dimension can be described by the simplified form of Fourier's Law in Equation 2:

$$q_x = -\lambda A (\Delta T/d) \tag{2}$$

Thermal conductivity of the samples was measured by means of a heat flow meter apparatus. The working of the apparatus is built upon the application of Fourier's Law, by generating one-directional heat flux across both surfaces of the specimen. The apparatus consists of a cold/hot plate, heat flux sensors and thermocouples. Thermal conductivity was determined from the measured heat flux and the temperature difference between the hot and cold sides of the

samples. Figure 4(a) shows the image of the apparatus in which the specimen is placed on top of the cold plate and T-type thermocouples attached on both surfaces of the specimen to measure temperature. The top surface is exposed to standard room conditions. The sample was allowed to stabilise for a certain time period before the heat flux was measured. Standard guarded hot plate method and Heat flow meter methods used to measure the thermal conductivity of insulation materials as described in BS EN 12667:2001 (BSI, 2001) require that both surfaces of the sample are exposed to controlled conditions by hot and cold plates. However, in these tests, the technique used allows comparable data to determine the thermal conductivity of the insulation material. Main purpose of testing the VIP for thermal conductivity using this comparative technique was to confirm the integrity of the VIP samples before using them in CIPs.

**[Figure 4 near here]**

Hukseflux heat flux sensors, Type HFP01, 80 mm diameter and 5 mm thick, were attached to the specimen on the top surface to measure the heat flux across the specimen. Performance of the apparatus was analysed by measuring the thermal conductivity of a 25 mm thick sample XPS (180 mm × 130 mm) of known thermal conductivity ( $33 \text{ mWm}^{-1}\text{K}^{-1}$ ). Thermal conductivity of the reference sample was measured to be  $31.91 \text{ mWm}^{-1}\text{K}^{-1}$ . This shows that the apparatus can measure thermal conductivity with good accuracy.

#### ***4.2 Thermal transmittance measurement of CIPs***

The  $U$ -value of a building element can be calculated from thermal resistances of the material layers and surface resistance of adjacent air layers. The thermal resistance of any layer can be obtained by dividing its thickness by thermal conductivity. In this study,  $U$ -value calculations are limited to only single panel and does not consider the panel-to-panel edge joints (the focus

was on improving the thermal and acoustic characteristics of a single panel; establishing the performance of a number of panels in a façade is outside the scope of this paper). However, for the purpose of the panel design system,  $U$ -value calculations should take into account the thermal effect of panel-to-panel edge (Nussbaumer, Wakili, Tanner , 2006) and fasteners which can cause higher heat losses. For a single panel, the equation given in BS EN 14509:2013 (BSI, 2013a) can be modified for flat profiled panel as shown in Equation 3.

$$U = 1/(R_{si} + \frac{t_i}{\lambda_{fi}} + \frac{d_c}{\lambda_c} + \frac{t_e}{\lambda_{fe}} + R_{se}) \quad (3)$$

For the  $U$ -value calculation, values of  $0.13 \text{ m}^2\text{KW}^{-1}$  and  $0.04 \text{ m}^2\text{KW}^{-1}$  were used for  $R_{si}$  and  $R_{se}$  respectively (CIBSE, 2015).

Thermal transmittance ( $U$ -value) of building elements in-situ can be determined using the average method by dividing the measured average heat flux by the mean temperature difference between the two sides of the element and measurements are taken over a period of time.  $U$ -value can be written as shown in Equation 4 as given in BS ISO 9869-1:2014 (BSI,2014a):

$$U = \frac{\sum_{j=1}^n q_j}{\sum_{j=1}^n (T_{ij} - T_{ej})} \quad (4)$$

where index  $j$  represents the individual measurement reading and  $T_i$  and  $T_e$  are the internal and external temperature respectively.

To determine the  $U$ -value of a CIP, the average heat flow passing through the CIP installed in the laboratory setup as shown in the Figure 4(b) was measured along with the surface temperature of both sides of the CIP. The same heat flux sensors used in Section 4.1 were employed in this test. T-Type thermocouples for temperature measurement were attached to

both surfaces of the CIP using strong adhesive tape to achieve good thermal contact. The heat flux data and temperature data was logged on a dataTaker DT85 data logger. Preferably, conditions on both sides of the CIP need to be as constant as possible. Although the laboratory room temperature was maintained, however fluctuations were expected during day time due to the ongoing activities in the laboratory. To ensure the steady state conditions, 48 hours of data obtained over a weekend was used for  $U$ -value calculations where temperature fluctuations were minimal. This test setup comparatively measures the  $U$ -value close to in-situ measurement which excludes the frame/fasteners. Once an optimised design is achieved, accredited testing of the best performing panel can be conducted in the guarded hot-box apparatus.

#### ***4.3 Sound transmission loss measurement of CIPs***

Sound transmission loss of can be measured in the laboratory by the two room method (Cavanaugh, 2010; Tadeu & Mateus, 2001). The requirements for accredited testing are based on BS EN 10140-5:2010+A1:2014 (BSI, 2014b) where information on the test facilities and equipment is given. It is stated that the volumes of the two test rooms shall be at least  $50\text{m}^3$ , which corresponds to a cubic room with dimensions of almost 3.7m. Therefore, due to the volumes of the reverberant rooms required, a very specialised test facility is required to fully comply with the test standard. Researchers elsewhere have recognised this issue and have investigated the possibility of using smaller scale test facilities for pre-compliance testing (del Rey et al., 2017; del Rey Tomos et al, 2015). Their aim was to strike a balance between reducing sample size and manufacturing costs of materials, and finding the appropriate volume of the chamber, to obtain reliable values at high and mid frequencies. The small-sized reverberation chamber, that was built, has a volume of  $1.12\text{ m}^3$  and allows for the testing of samples of  $0.3\text{ m}^2$ . Several comparison studies in the small-sized reverberation chamber and those in the standardised reverberation chamber were carried out. The measurements of the

small-sized chamber coincided well with the measurements of the standardised chamber, in the range of frequencies in which the small-sized reverberation chamber fulfils the diffusion conditions. Their conclusion was that the small-sized reverberation chamber permits the testing and comparison of small samples of materials, so that a few of them can later be chosen to be tested in a standardised reverberation chamber. Elsewhere, Walters and Dance (2014) used smaller chamber dimensions (actual chamber sizes were not given but the test panel was  $0.54\text{m}^2$ ). They showed that after several modifications and retesting, it was concluded that the performance of the control enclosure performed as good as one of the most expensive commercial offerings.

Since one of the aims of this paper was to develop enhanced VIC panels with enhanced acoustic performance, the two room method was also employed in this study to comparatively measure the sound transmission of multi-layered panels but in a laboratory scale facility consisting of specially prepared twin chambers shown in Figure 5 (a). Sizes of the test chambers are given in Figure 5 (b). Their smaller size provided a more convenient and affordable test environment for product design and development applications with reliable outputs to comparatively screen the different designs.

**[Figure 5 near here]**

Volumes of the receiver and source chambers were  $0.61\text{ m}^3$  and  $0.85\text{ m}^3$  respectively and dimensions of the opening were  $0.566\text{ m}$  by  $0.566\text{ m}$ . NTI XL2 acoustic analyser and M2230 Class 1 microphone were used for sound pressure level measurements and were fully certified (all acoustic test equipment was bought specifically for the testing). Omni-directional speaker of  $90\text{ mm}$  diameter, power output of  $1.5\text{ W}$  and frequency response of  $80\text{ Hz}$ - $18\text{ kHz}$  was used as a sound source. Sound pressure level was measured in the receiver and source rooms, each at three different locations at least  $250\text{ mm}$  away from each other for six seconds. Average

background sound pressure level in the receiver room was measured for 18 seconds. Reverberation time was measured using hand clap as impulse source without installing the sample in the chamber. Seetharaman & Tarzia (2012) has described the hand clap as an Impulse source a reliable method for measuring reverberation time. Measured reverberation time in the receiver chamber was an average of three measurements at one microphone location (Alam & O'Flaherty, 2016). Sound reduction index ( $R$ ) was calculated using Equation 5 (BSI, 2010).

$$R = L_s - L_r + 10 \log(S/A_e) \quad (5)$$

$A_e$  can be calculated using the Sabine formula  $A_e = 0.161 \times \left(\frac{V}{t}\right)$ . Sound source, chamber absorbing conditions, location of microphone and measurement averaging time remained unchanged during all experimental measurements.

Sound reduction index ( $R$ ) is measured at various frequencies, generally one-third octave band between 100 Hz and 3150 Hz. However, a single number rating i.e. weighted sound reduction index ( $R_w$ ) is required for quantitatively measuring the sound insulation properties of each panel.  $R_w$  can be calculated using the procedure described in BS EN ISO 717-1 (BSI, 2013b) where measured results are compared against the reference curve given in BS EN ISO 717-1. The reference curve is shifted towards the measured curve in increments of 1 dB until the total of unfavourable deviations is as large as possible but not more than 32 dB. An unfavourable deviation at a particular frequency takes place when the experimental  $R$  value is lower than the reference curve value. The value of shifted reference curve value at 500 Hz frequency is considered as the weighted sound reduction index,  $R_w$ .

## 5 Results and discussion

### 5.1 Thermal conductivity of vacuum insulation

The thermal conductivities of two commercially available vacuum insulation samples (VIP1 and VIP2) with the same composition have been measured using apparatus described in Section 4.1. The results of measured thermal conductivity (taken at the centre of the panel) of the tested VIP samples are presented in Table 3. Thermal conductivity values of 4.31 and 3.91  $\text{mWm}^{-1}\text{K}^{-1}$  were measured for specimens VIP1 and VIP2 respectively. The manufacturer's thermal conductivity values were given as 4.7  $\text{mWm}^{-1}\text{K}^{-1}$  (centre of panel). Hence, the samples VIP1 and VIP2 performed slightly better in the laboratory test. Capozzoli et al. (2015) identified that small variation in measured centre of panel thermal conductivity values can arise due to small changes in surface thermal contact resistance. This was due to the uneven surface of the panels and small variation in the degree of vacuum from VIP to VIP. By using a standardised guarded hot plate method, VIP thermal conductivity values varied from 2.6  $\text{mWm}^{-1}\text{K}^{-1}$  to 4.7  $\text{mWm}^{-1}\text{K}^{-1}$  for theoretically identical commercially available VIP samples (Capozzoli et al., 2015). The centre of panel thermal conductivity values of the commercially available VIP measured in this study (4.31 and 3.91  $\text{mWm}^{-1}\text{K}^{-1}$ ) are comparable to those measured by the guarded hot plate method and therefore, indicates the validity of the comparative test method used in this study.

Furthermore, these results show that the vacuum insulation used in the CIP manufacturing were intact and not damaged during transportation and handling. Taking an average value of 4.11  $\text{mWm}^{-1}\text{K}^{-1}$ ,  $\lambda$  for the vacuum insulation is 7.8 times lower than the equivalent value for XPS (31.91  $\text{mWm}^{-1}\text{K}^{-1}$ ). The manufacturer's declared aged design value is 7  $\text{mWm}^{-1}\text{K}^{-1}$  for these VIPs which takes into account both edge and ageing effects. This confirms that heat loss increases at the edges compared to the centre of the panel. This effect will be more pronounced

in the VIC panels with an XPS border for puncture protection and this is considered in Section 5.2.

**[Table 3 near here]**

### ***5.2 Effect of vacuum insulation on thermal performance of CIPs***

Results of  $U$ -values of CIP panel samples were determined from measurements taken at the edge and centre of the CIP panels. Figure 4 (b) shows the setup of  $U$ -value measurement at the centre of panel. For measurement of the edge  $U$ -value, additional heat flux sensors and thermocouples were attached to samples at the edge of the panels. CIP made with vacuum insulation core (Panel T2) at the centre had an average  $U$ -value of  $0.38 \text{ Wm}^{-2}\text{K}^{-1}$  compared to that of  $0.78 \text{ Wm}^{-2}\text{K}^{-1}$  for the XPS core control panel (Panel T1), see Figure 6. This shows that the presence of vacuum insulation has improved the thermal performance of CIP (Panel T2) by reducing the  $U$ -value by  $0.40 \text{ Wm}^{-2}\text{K}^{-1}$ , a 51% improvement in thermal performance compared to that of CIP with XPS core (Panel T1). Therefore, the thickness of XPS would have to be more or less doubled to achieve a similar performance compared to that of the vacuum insulation in the centre of the panel.

**[Figure 6 near here]**

Considering the centre of panel vacuum insulation core thermal conductivity of  $4.11 \text{ mWm}^{-1}\text{K}^{-1}$ , the  $U$ -value at centre of panel of CIP was theoretically expected to be around  $0.20 \text{ Wm}^{-2}\text{K}^{-1}$ . However, small size of VIPs used in this study and edge effect due to the individual panel and air gap between two VIPs led to a negative effect on the  $U$ -value of panel and a higher  $U$ -value of  $0.38 \text{ Wm}^{-2}\text{K}^{-1}$  was obtained in this investigation. The increase in thermal conductivity for small vacuum insulation panel can easily be between 11% and 15% higher than the centre of panel thermal conductivity (Sprengard & Holm 2014). Edge effect due to air gap between small VIPs can also reduce the thermal resistance and the practical equivalent thermal

conductivity value was measured to be about  $8 \text{ mWm}^{-1}\text{K}^{-1}$  for panel size  $300 \text{ mm} \times 300\text{mm}$  (Lorenzati, Fantucci, Capozzoli, Perino, 2015).

Data also shows that the  $U$ -values at the edge of the CIP were found to be higher compared to that at the centre of the CIP (Figure 6 and Table 4). For CIPs with vacuum insulated core, the edge  $U$ -value was measured to be  $0.64 \text{ Wm}^{-2}\text{K}^{-1}$  (an increase of 68%, Table 4) while for the CIP with XPS was  $0.97 \text{ Wm}^{-2}\text{K}^{-1}$  (an increase of 24%, Table 4). This edge effect is, therefore, greater for the CIP with vacuum insulated core due to the low thermal conductivity of the vacuum insulation core. The two options available to improve this situation are: (i) remove the XPS border completely and increase the size of the VIC; (ii) minimise the impact of the XPS through considered design. Option (i) puts the durability of the VIC at risk of puncture and may also lead to increase in the edge effect if the VIC comes in direct contact with surrounding panel or frame. Due to the risks of puncture and deterioration of performance as a result of possible edge effect, it is imperative that the XPS border remains. Option (ii) retains the XPS border but a compromise has to be made. A trade-off is made by accepting a lower performance but its effect can be minimised by considering the design recommendations given in Section 5.3.

**[Table 4 near here]**

### ***5.3 Design considerations for CIPs with vacuum insulation core***

The significantly higher  $U$ -value at the edges of the CIP with vacuum insulation requires that the overall size of these panels and edges should be designed very carefully in order to effectively utilise the enhanced thermal performance of the vacuum insulation in the CIP. This edge effect could potentially be reduced by increasing the vacuum insulated core area and reducing the edge width and/or using low thermal conductivity foams such as phenolic foam

or polyurethane foam instead of XPS. However, the protective border needs to be of a certain size so protection is offered to the VIC. As identified previously in Section 5.2, the edge effect has a greater influence on CIP  $U$ -value and needs to be included in CIP design calculations. For design purposes in this study, composite  $U$ -values were calculated from measured centre of CIP  $U$ -values and edge  $U$ -values for different panel sizes taking into account the area of panel covered by the vacuum insulation of 20 mm thickness and XPS edge. A practical XPS edge width of 25 mm was assumed for the design calculations. Composite  $U$ -values for the vacuum insulation CIPs with different vacuum insulated core areas are shown in Figure 7. Referring to Figure 7, five different total panel areas are considered (0.119, 0.812, 1.562, 3.600 and 4.800 m<sup>2</sup>). Using the XPS border of 25mm to protect the vacuum insulation, the net area of vacuum insulation is obtained.

**[Figure 7 near here]**

The calculated values illustrate that a vacuum insulated area of 0.087 m<sup>2</sup> in an overall panel size of 0.119 m<sup>2</sup> resulted in a  $U$ -value of 0.45 Wm<sup>-2</sup>K<sup>-1</sup>. Increasing the vacuum insulated area to 0.720 m<sup>2</sup> in an overall panel size of 0.812 m<sup>2</sup> resulted in the  $U$ -value decreasing to 0.41 Wm<sup>-2</sup>K<sup>-1</sup>, an improvement of 0.04 Wm<sup>-2</sup>K<sup>-1</sup>. Doubling the vacuum insulated area to 1.440 m<sup>2</sup> led to the  $U$ -value of 0.40 Wm<sup>-2</sup>K<sup>-1</sup>, a decrease of only 0.01 Wm<sup>-2</sup>K<sup>-1</sup> compared to the vacuum insulated area of 0.720 m<sup>2</sup>. Increasing the vacuum insulated area to 3.393 m<sup>2</sup> resulted in further improvement of only 0.01 Wm<sup>-2</sup>K<sup>-1</sup>. The  $U$ -value remains at 0.39 Wm<sup>-2</sup>K<sup>-1</sup> when the vacuum insulation area is increased to 4.543 m<sup>2</sup> in an overall panel area of 4.800 m<sup>2</sup>. This shows that the vacuum insulated core area in the CIP between the range of say 0.75 m<sup>2</sup> and 3.5 m<sup>2</sup> will yield an optimal thermal performance. Large vacuum insulated area in CIP will be preferred resulting in smaller perimeter to surface ratio. Lower perimeter to surface ratio of vacuum insulated core will result in lower edge effect. Specifying panels with areas below 0.75 m<sup>2</sup> results in a reduced thermal performance; specifying panels with areas greater than 3.5 m<sup>2</sup> is

also possible but it would not lead to an increased thermal performance and handling and manufacturing difficulties may ensue.

#### ***5.4 Influence of MLV layer on sound insulation performance of XPS core CIPs***

Measured value of sound reduction index ( $R$ ) of XPS core CIP Panels A1, A2 and A3 (AXA, AMXA and AMXMA respectively, Table 2) are shown in Figure 8. It is evident that the presence of the MLV layer has led to an increase in the  $R$  values of CIP prototypes Panels A2 and A3 (AMXA and AMXMA respectively) in comparison to that of MLV-free AXA prototype (Panel A1). Panel A3 (AMXMA) was found to perform better in tests due to the presence of two MLV layers leading to an increase in weight and damping effect compared to the other two prototypes. The weight increased from  $9.4 \text{ kg/m}^2$  for Panel A1 (AXA) prototype to  $19.2 \text{ kg/m}^2$  in Panel A3 (AMXMA) prototype. However, all prototype CIPs show a dip in sound insulation starting around 2000 Hz, probably due to the coincidence effect which takes place when the wavelength of bending waves in the panel is the same as the wavelength of the airborne sound waves.

**[Figure 8 near here]**

$R_w$  values of samples along with panel weights are shown in Figure 9. It was found that the sound insulation of CIPs increased with increasing weight. In the case of control CIP No. A1 (AXA) with a weight of  $9.4 \text{ kg/m}^2$ ,  $R_w$  was 35 dB. By adding a single MLV layer, the weight of CIP prototype No. A2 (AMXA) increased to  $13.8 \text{ kg/m}^2$  and  $R_w$  value increase by 3 dB. In the case of CIP prototype No. A3 (AMXMA) with two MLV layers  $R_w$  value was found to be 39 dB, an increase of only one dB compared to prototype No. A2 (AMXA). However, comparison of control prototype No. A1 (AXA) and prototype No. A3 (AMXMA) shows that the weight has approximately doubled whereas the total  $R_w$  value improved by 4 dB. This is slightly less than what would be expected by the Mass Law where a 6 dB improvement in  $R_w$

value is expected for each doubling of mass. This behaviour can be attributed to the location of the second MLV layer in Panel A3 (AMXMA). In CIP prototype No. A2 (AMXA), one MLV layer was attached inside the aluminium skin directly facing the sound source and resulted in an increase in  $R_w$  of 3 dB. This aligns with the Mass Law as the weight of CIP increased by 47%. However, in Panel A3 (AMXMA), the second MLV layer was attached inside the opposite aluminium skin not directly facing the sound source and resulted in only a 4 dB improvement in  $R_w$  while the weight increased roughly twofold (by 104%) in comparison to CIP prototype No. A1 (AXA). This demonstrates that it would be beneficial to attach a single heavier MLV layer at the CIP skin directly facing the sound source compared to two lighter MLV layers acting as damping layer at either face of the CIP.

**[Figure 9 near here]**

### ***5.5 Effect of MLV layer on sound insulation performance of vacuum insulated core CIPs***

Comparison of sound reduction index ( $R$ ) measurement of CIP No. A4 (AXVXA) i.e. without any MLV layer and No. A5 (AMVMA) i.e. two MLV layers each side of vacuum insulation core is shown in Figure 10. Results indicate that the presence of the MLV layers has led to higher  $R$  values for Panel A5 with MLV membranes compared to that of MLV-free Panel A4 in the lower frequency range of 125 Hz to 630 Hz. Panel A4 (AXVXA) has shown slightly better performance in the frequency range of 1600 Hz to 3150 Hz. However, both panels show a coincidence dip around 800 - 1000 Hz which lies in the peak road traffic noise third-octave frequency bands between 800 and 1250 Hz. This dip needs to be shifted out of the frequency range of 100 - 3150 Hz to achieve better sound insulation values. The effect of coincidence dip could possibly be reduced or eliminated by achieving perfect contact between MLV layers and other layers (VIC and aluminium skin) in the panel.

**[Figure 10 near here]**

Weighted sound reduction value and weight comparison of vacuum insulated CIPs are shown in Figure 11. Integration of MLV layers has led to increase in the total weight of the panel. However, the weighted sound reduction index increase of only 3 dB is approximately 3dB lower than what would be expected through the Mass Law. However, a similar shortfall of approximately 3dB has also been measured by Maysenhölder (2008) for façade panels made using vacuum insulation cores. Maysenhölder (2008) attributed this anomaly to the gluing deficiencies in the façade panel. It is required that panel behaves as single component to follow the Mass Law. This may well be the case in this study as it was difficult to achieve a perfect bond between the MLV, aluminium and vacuum insulated core due to the envelope seam folded back on one side of the vacuum insulation leading to an uneven surface on the vacuum insulated core. It will be beneficial to use vacuum insulation with a smooth surface where the envelope seams are folded back on the edges rather than on one face of the vacuum insulation to achieve better bonding. However, the other possible reason can be the position of MLV layer in Panel A4 (AMVMA) where one MLV layer is facing away from the sound source. This implies that it would be beneficial to add a heavier MLV layer equivalent of two lighter MLV layers facing the sound source to achieve better sound insulation performance as also shown in the XPS core panels in Section 5.4. Aluminium was considered as the facing material due to it being a commonly used façade material. Facing materials with higher density e.g. steel will be expected to show higher sound insulation performance due to their higher weight as expected by the Mass Law but at the cost of increased panel weight.

**[Figure 11 near here]**

## **6 Conclusions**

This paper reports the development of smart façade panels using vacuum insulation core (VIC) combined with mass loaded vinyl (MLV) membranes with the purpose of achieving higher thermal and sound insulation. Testing was done in a small scale laboratory acoustic chambers

as this provided a more convenient and affordable test environment for product design and development applications ahead of accredited testing based on BS EN 10140. The use of vacuum insulation core serves to improve the thermal insulation properties while MLV layers offer the sound insulation. Comparatively, the thermal transmission ( $U$ -value) at the centre of the composite insulation panels with VIC was measured to be  $0.38 \text{ Wm}^{-2}\text{K}^{-1}$  compared to that of  $0.78 \text{ Wm}^{-2}\text{K}^{-1}$  for extruded polystyrene (XPS) core control panel. This 51% improvement in  $U$ -value was attained without any significant change in the overall thickness of the CIP. Achieving similar performance with XPS core panel would have required almost two-fold increase in the thickness of the panel. However, at the edge of the panel a 68% increase in  $U$ -value from  $0.38 \text{ Wm}^{-2}\text{K}^{-1}$  to  $0.64 \text{ Wm}^{-2}\text{K}^{-1}$  was measured due to higher thermal conductivity of XPS border used for VIC edge protection. This higher  $U$ -value at the edge of the panel can be minimised by increasing the area of vacuum insulation core in the panel. It was calculated that the vacuum insulated core area of  $3.393 \text{ m}^2$  in an overall panel area of  $3.6 \text{ m}^2$  could yield a composite  $U$ -value (including edge and centre values) of  $0.39 \text{ Wm}^{-2}\text{K}^{-1}$  only  $0.01 \text{ Wm}^{-2}\text{K}^{-1}$  higher than the centre of panel value of  $0.38 \text{ Wm}^{-2}\text{K}^{-1}$ . Integration of thin MLV layers inside of both aluminium skins of vacuum insulated core panel led to 3 dB increase in weighted sound reduction index ( $R_w$ ) values compared to that of MLV free panels. The VIC panel with two MLV membranes were found to have the  $R_w$  of 35 dB compared to values of 32 dB for panel without any MLV layers. It has been found that both XPS and VIC core panels show a different behaviour to that of Mass Law, a comparison that is commonly made by researchers.  $R_w$  values were 2-3 dB below what was expected of the Mass Law values. It was found that integrating one heavier layer inside the aluminium skin facing the sound source had higher  $R_w$  values for XPS panels compared to the panels having two lighter MLV layers on either side of XPS core panel. This is also applicable to VIC panels, the position of one heavier layer inside the aluminium skin facing the sound source can further improve the sound insulation. Moreover,

in the case of VIC panels achieving better surface bonding between MLV and vacuum insulation for panel to behave as a single component is expected to further enhance the sound insulation. This comparative study shows that it is possible to develop smart facade panel solutions using vacuum insulation combined with MLV layers to achieve better thermal and sound insulation properties without any adverse effect on the overall thickness of the panel.

### **Disclosure statement**

No potential conflict of interest was reported by the authors

### **Acknowledgements**

This work was financially and technically supported by Innovate UK and Panel Systems Limited, Sheffield (Knowledge Transfer Partnership (KTP) Programme, No. 009433, 2014-2016)

**Declarations of interest:** None

**Word Count:** 6520

### **8 References**

Alam M., O’Flaherty F. (2016). Influence of acoustic membrane on sound and thermal properties of building façade panels. In: 11th Conference on Advanced Building Skins, Bern, Switzerland, 10-11 October 2016. Switzerland, Advanced Building Skins GmbH.

Alam M., Singh H. and Limbachiya M.C. (2011). Vacuum Insulation Panels (VIPs) for building construction industry - A review of the contemporary developments and future directions, *Applied Energy*, 88, 3592 - 3602.

Alam M., Singh H. Suresh S. and Redpath D.A.G. (2017). Energy and economic analysis of Vacuum Insulation Panels (VIPs) used in non-domestic buildings, *Applied Energy* 188, 1-8.

Azimi M. (2017). Noise Reduction in Buildings Using Sound Absorbing Materials. *Journal of Architectural Engineering and Technology*, 6: 198.

Baetens R., Jelle B.P., Thue J.V., Tenpierik M.J., Grynning S., Uvsløkk S., Gustavsen A.. (2010) Vacuum Insulation Panels for Building Applications: A Review and Beyond. *Energy and Buildings*, 42,147-172.

- Ballagh K.O. (2010). Adapting Simple Prediction Methods to Sound Transmission of Lightweight Foam Cored Panels. Proceedings of the International Symposium on Sustainability in Acoustics, 29-31 August 2010, Auckland, New Zealand.
- Biswas K., Desjarlais A., Smith D. Letts J., Yao J., Jiang T. (2018). Development and thermal performance verification of composite insulation boards containing foam-encapsulated vacuum insulation panels. *Applied Energy*, 228, 1159-1172
- British Standards Institute- BSI, (2001). BS EN 12667:2001. Thermal performance of building materials and products. Determination of thermal resistance by means of guarded hot plate and heat flow meter methods. Products of high and medium thermal resistance
- British Standards Institute- BSI, (2010). BS EN ISO 10140-2:2010. Acoustics — Laboratory measurement of sound insulation of building elements Part 2: Measurement of airborne sound insulation.
- British Standards Institute-BSI (2013a). BS EN 14509:2013. Self-supporting double skin metal faced insulating panels — Factory made products — Specifications.
- British Standards Institute-BSI (2013b). BS EN ISO 717-1:2013. Acoustics- Rating of sound insulation in buildings and of building elements Part 1: Airborne sound insulation.
- British Standards Institute -BSI (2014a) BS ISO 9869-1:2014 Thermal insulation - Building elements - In-situ measurement of thermal resistance and thermal transmittance
- British Standards Institute- BSI, (2014b). BS EN ISO 10140-5:2010+A1:2014. Acoustics — Laboratory measurement of sound insulation of building elements Part 5: Requirements for the test facilities and equipment
- Brunner S. and Simmler H. (2008). In situ performance assessment of vacuum insulation panels in a flat roof construction. *Vacuum*, 82, 700-707.
- Capozzoli A., Fantucci S., Favoino F. and Perino M. (2015). Vacuum Insulation Panels: Analysis of the Thermal Performance of Both Single Panel and Multilayer Boards. *Energies*, 8, 2528-2547.
- Cauberg H and Tenpierik M. (2007). Sound reduction of vacuum insulation based on building panels. In: Proceedings of 19<sup>th</sup> International congress on acoustics. Madrid, Spain. 2-7 September 2007.
- Cavanaugh W.J. (2010) Introduction to architectural acoustics and basic principles. In: Cavanaugh W.J., Tocci G.C. & Wilkes J.A (eds.). *Architectural acoustics: Principles and practice*. 2nd edition, John Wiley & Sons, New Jersey, 1-32.
- Chartered Institution of Building Services Engineers (CIBSE) (2015). *Environmental design-CIBSE Guide A*. Eighth edition; The Chartered Institution of Building Services Engineers, London.
- Davies J.M., (2001). *Lightweight sandwich construction*. Blackwell Science, Oxford.
- del Rey, R., Alba, J., Bertó, L., Gregori, A., Small-sized reverberation chamber for the measurement of sound absorption, *Materiales de Construcción*, Vol 67, No 328 (2017). <http://materconstrucc.revistas.csic.es/index.php/materconstrucc/article/view/2195/2764>. Accessed 25 July 2018
- del Rey Tormos, R., Bertó, L., Alba Fernandez, J. Arenas, J. (2015). Acoustic characterization of recycled textile materials used as core elements in noise barriers, *Noise Control Engineering*, 63(5):439-447. DOI: 10.3397/1/376339

- European Commission (2017). <https://ec.europa.eu/energy/en/topics/energy-efficiency/buildings> [accessed 13 December 2107]
- Hayez V. and Kragh M. (2013). Next generation curtain walling: Using vacuum insulation panels - energy performance and design freedom. *Façade Tectonics Journal*, 17, 19-30.
- Kan A. and Hu J. (2017). Thermal performance evaluation on vacuum insulation panels in composite building envelope under large temperature variations. *International Journal of Low-Carbon Technologies*, 12, 51-53.
- Long M. (2014). *Architectural Acoustics*, 2nd end. Elsevier Academic Press. Oxford.
- Lorenzati A., Fantucci S., Capozzoli A. and Perino M. (2016). Experimental and numerical investigation of thermal bridging effects of jointed Vacuum Insulation Panels. *Energy and Buildings*, 111, 164-175.
- Mandilaras I., Atsonios I., Zannis G. and Founti M., (2014). Thermal performance of a building envelope incorporating ETICS with vacuum insulation panels and EPS. *Energy and Buildings*, 85, 666-671.
- Maysenhölder (2008). Sound transmission loss of vacuum insulation panels. In: proceeding of Acoustic08, 29 June - 4 July, 2008, Paris, France.
- Nussbaumer T., Wakili K.G. and Tanner C. (2006). Experimental and numerical investigation of the thermal performance of a protected vacuum-insulation system applied to a concrete wall. *Applied Energy*, 83, 841-855.
- Praščević, M., Cvetković, D., & Mihajlov, D. (2012). Comparison of prediction and measurement methods for sound insulation of lightweight partitions. *Facta Universitatis – Series: Architecture and Civil Engineering*, 10, 155–167.
- Seetharaman, P., & Tarzia, S. P. (2012, April). The hand clap as an impulse source for measuring room acoustics. 132nd Audio Engineering Society Convention, Budapest, Hungary.
- Sprengard C. and Holm H. A. (2014). Numerical examination of thermal bridging effects at the edges of vacuum-insulation-panels (VIP) in various constructions. *Energy and Buildings*, 85, 638-643.
- Tadeu A.J.B. and Mateus D.M.R. (2001). Sound transmission through single, double and triple glazing. Experimental evaluation. *Applied Acoustics*, 62,307-325.
- Voellinger T., Bassi A., Heitel M. (2014). Facilitating the incorporation of VIP into precast concrete sandwich panels. *Energy and Buildings*, 85, 666-671.
- Wakili K.G., & Bundi, R. and Binder, B. (2004). Effective thermal conductivity of vacuum insulation panels. *Building Research and Information*, 32, 293-299.
- Walters, S., Dance, S., Noise control potential of vacuum isolation panels, Inter noise 2014, Melbourne, Australia, 16-19 November, pp. 1-10
- Wareing R. R., Davy J. L. and Pearse J. R. (2015). Predicting the Sound Insulation of Plywood Panels When Treated with Decoupled Mass loaded Barriers, *Applied Acoustics*, 91, 64-72.

## List of Tables

**Table 1.** Composition and thickness of investigated CIP prototypes for thermal insulation testing

**Table 2.** Composition, weight and thickness of investigated CIP prototypes for sound insulation testing

**Table 3.** Measured thermal conductivity of vacuum insulation

**Table 4.** Comparison of U-values at centre and edge of CIPs

**Table 1.** Composition and thickness of investigated CIP prototypes for thermal insulation testing

No.	Proto-type*	Layers				Thickness (mm)	
		Facing	Core		Facing		
T1	AXA	Aluminium 1.5 mm	XPS 25 mm		Aluminium 1.5 mm	28	
T2	AXVX A	Aluminium 1.5 mm	XPS 3 mm	VIC 20 mm	XPS 3 mm	Aluminium 1.5 mm	29

\*The acronyms relate to the composition and number of layers in the sandwich panels, being a combination of Aluminium (A), XPS (X) and/or Vacuum insulation core (V)

**Table 2.** Composition, weight and thickness of investigated CIP prototypes for sound insulation testing

No.	Proto-type*	Layers					Weight (kg/m <sup>2</sup> )	Thickness (mm)
		Facing	Acoustic	Thermal	Acoustic	Facing		
A1	AXA	Aluminium 1.5 mm	-	XPS 25 mm	-	Aluminium 1.5 mm	9.4	28
A2	AMXA	Aluminium 1.5 mm	MLV 2.25 mm	XPS 22 mm	-	Aluminium 1.5 mm	13.8	27.25
A3	AMXMA	Aluminium 1.5 mm	MLV 2.25 mm	XPS 22 mm	MLV 2.25 mm	Aluminium 1.5 mm	19.2	29.5
A4	AXVXA	Aluminium 1.5 mm	XPS 3 mm	VIC 20 mm	XPS 3 mm	Aluminium 1.5 mm	11.9	29
A5	AMVMA	Aluminium 1.5 mm	MLV 2.25 mm	VIC 20 mm	MLV 2.25 mm	Aluminium 1.5 mm	21.3	27.5

\* The acronyms relate to the composition and number of layers in the sandwich panels, being a combination of either Aluminium (A), Mass Loaded Vinyl (M), XPS (X) or Vacuum insulation panel (V)

**Table 3.** Measured thermal conductivity of vacuum insulation

<b>Sample</b>	<b>Thickness (mm)</b>	<b>Dimensions (mm)</b>	<b>Mean Temperature (°C)</b>	<b>Thermal Conductivity (mWm<sup>-1</sup>K<sup>-1</sup>)</b>
VIP1	20	300 × 300	9.78	4.31
VIP2	20	300 × 300	9.76	3.91
				Average: 4.11

**Table 4.** Comparison of U-values at centre and edge of CIPs

<b>Panel No.</b>	<b>Prototype</b>	<b>Centre U- value (Wm<sup>-2</sup>K<sup>-1</sup>)</b>	<b>Edge U- value (Wm<sup>-2</sup>K<sup>-1</sup>)</b>	<b>Difference between Edge and centre (Wm<sup>-2</sup>K<sup>-1</sup>)</b>
<b>T1</b>	CIP with XPS	0.78	0.97	0.19 (+24%)
<b>T2</b>	CIP with vacuum insulation	0.38	0.64	0.26 (+68%)

## List of Figures

**Figure 1.** Layout and manufacturing of vacuum insulated composite insulation panel for thermal transmission testing (Panel T2). (a) XPS edge border placed on aluminium skin (b) XPS bottom layer placed on aluminium skin inside XPS borders (c) insertion of vacuum insulation cores (2 x 300mm x 300mm) (d) complete composite insulation panel after placing XPS top layer and aluminium skins

**Figure 2.** Layout of different layers of A-type panel samples

**Figure 3.** Layout and manufacturing of vacuum insulated composite insulation panel for sound insulation testing (Panel A4) (a) XPS edge border placed on aluminium skin (b) XPS bottom layer placed on aluminium skin inside XPS borders (c) insertion of vacuum insulation core (2 x 300mm x 300mm) (d) complete composite insulation panel after placing XPS top layer and aluminium skins

**Figure 4.** (a) Thermal conductivity measurement equipment (b)  $U$ -values measurement setup (centre of panel)

**Figure 5.** Sound insulation test setup: (a) Measurement setup during test; (b) Schematic of the setup

**Figure 6.** Measured  $U$ -values of CIPs made with vacuum insulation and XPS core

**Figure 7.** Composite  $U$ -values for the vacuum insulation CIPs with different vacuum insulated core areas

**Figure 8.** Measured sound reduction index ( $R$ ) for different prototype CIPS

**Figure 9.** Comparison of weight and measured weighted sound reduction index ( $R_w$ )

**Figure 10.** Effect of MLV layer on the sound reduction index ( $R$ ) of vacuum insulated CIPs

**Figure 11.** Measured weighted sound reduction ( $R_w$ ) and weight comparison of vacuum insulated CIPs



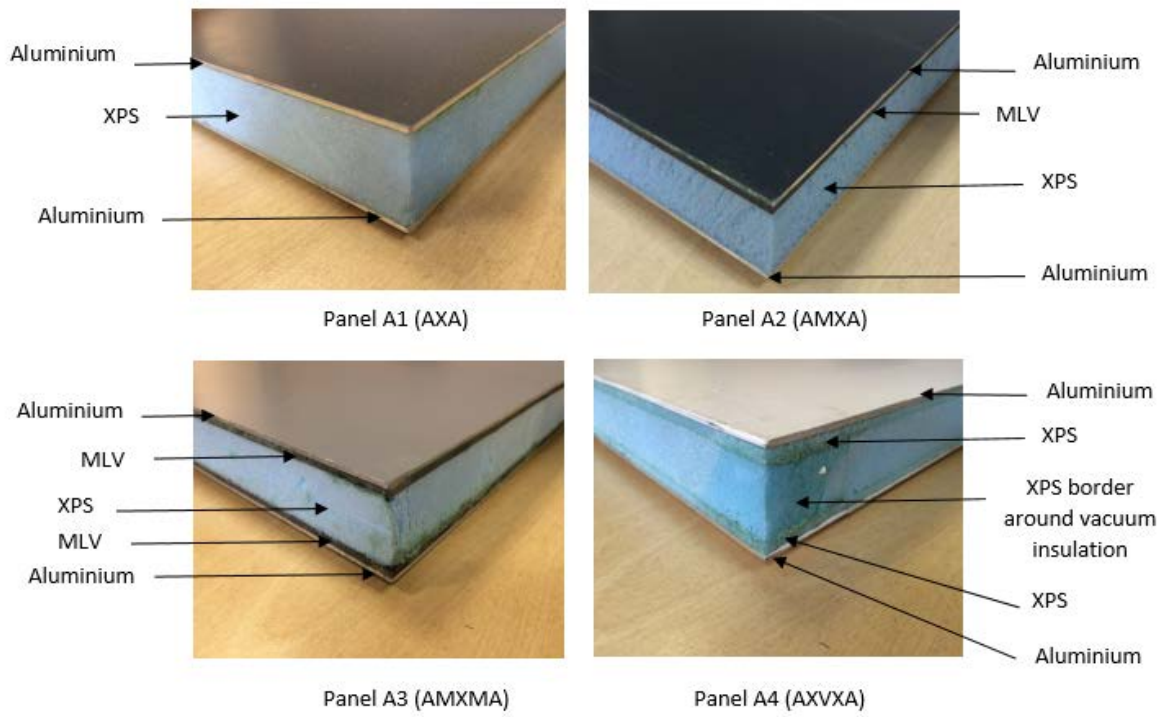


**Figure 2.** Layout of different layers of A-type panel samples



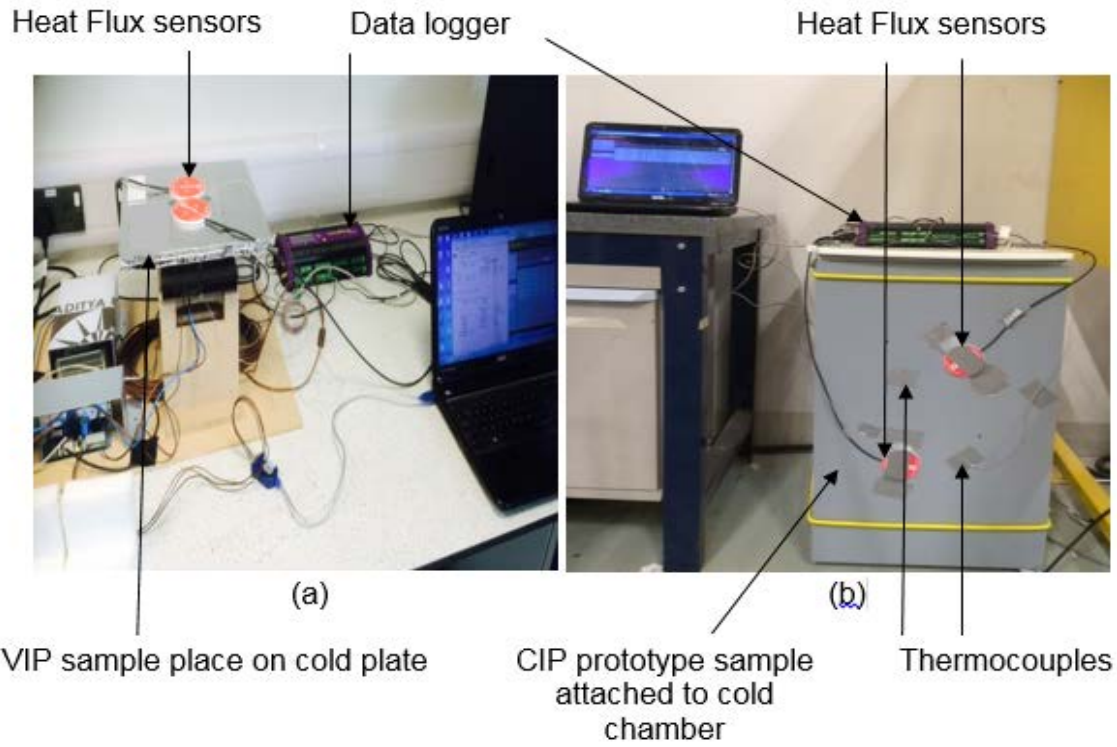
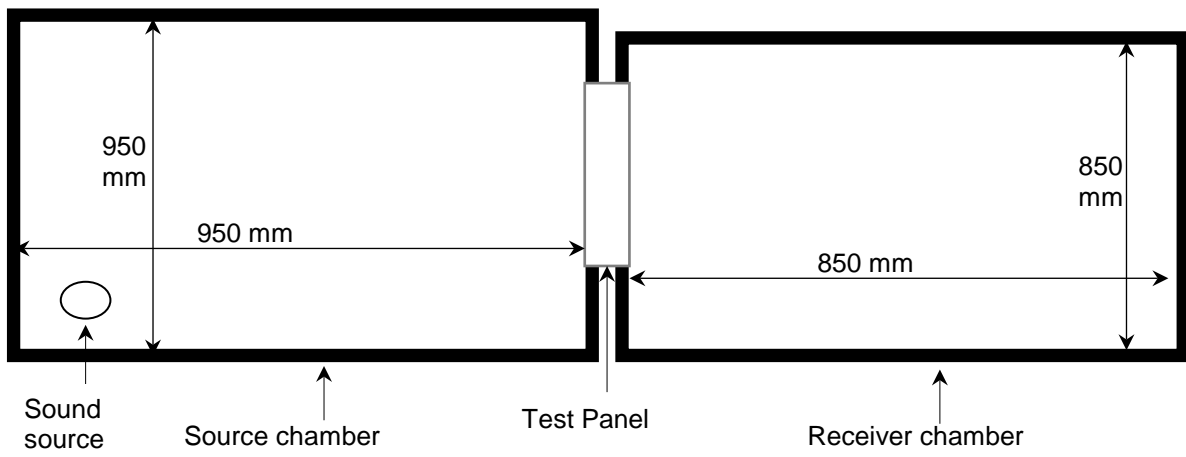


**Figure 4.** (a) Thermal conductivity measurement equipment (b)  $U$ -values measurement setup (centre of panel)



(a)



(b)

**Figure 5.** Sound insulation test setup: (a) Measurement setup during test; (b) Schematic of the setup

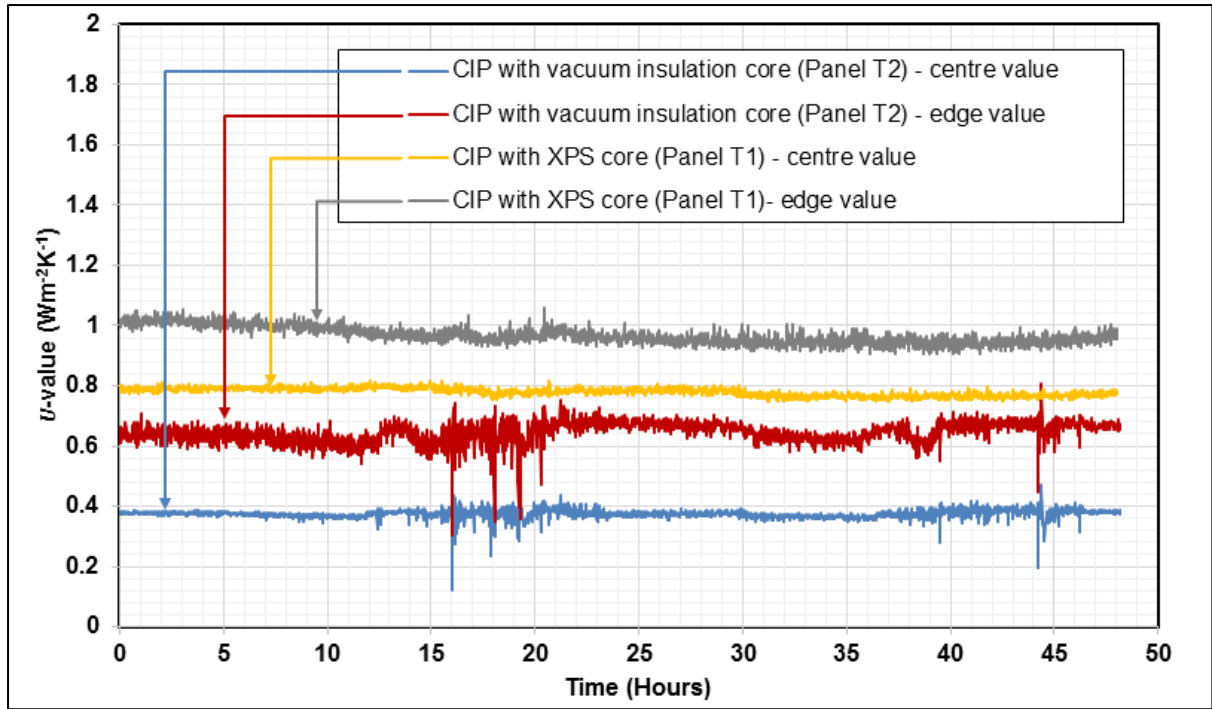


**Figure 6.** Measured U-values of CIPs made with vacuum insulation and XPS core

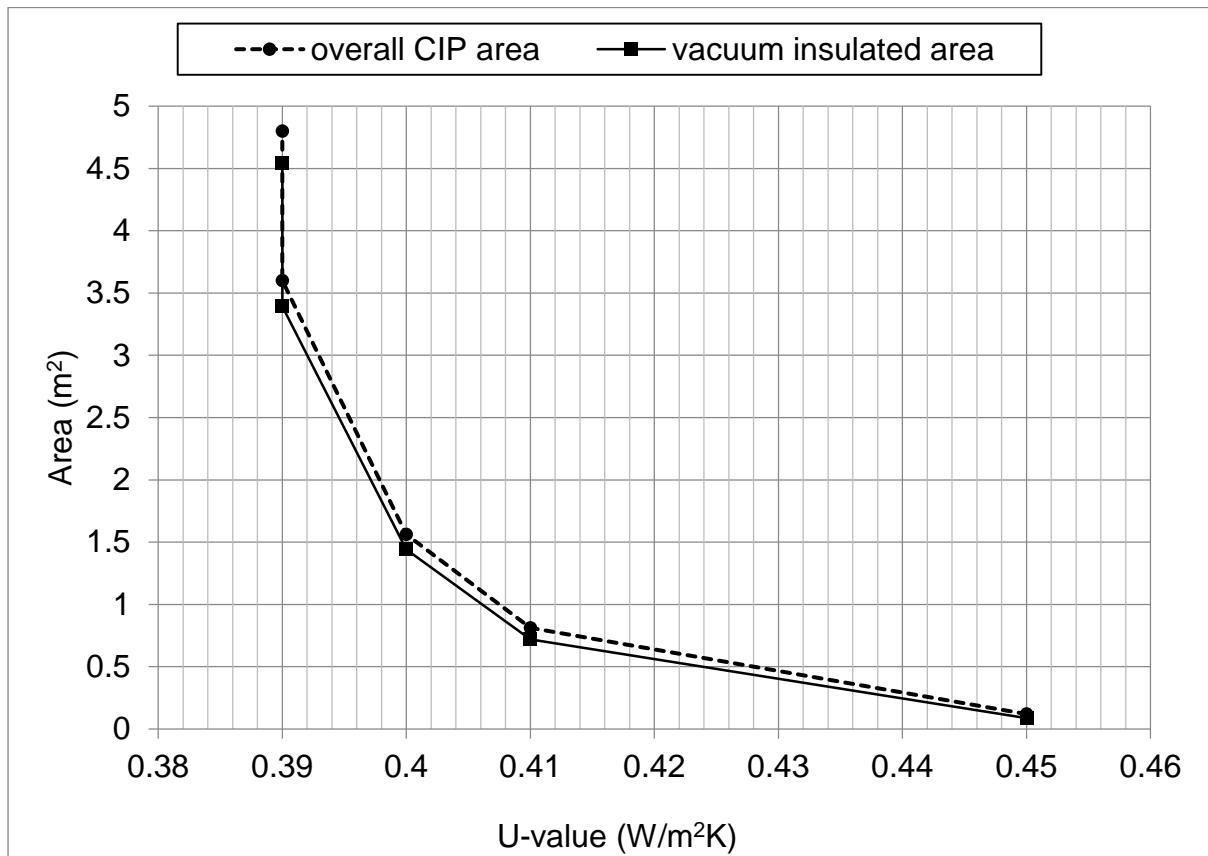


**Figure 7.** Composite U-values for the vacuum insulation CIPs with different vacuum insulated core areas

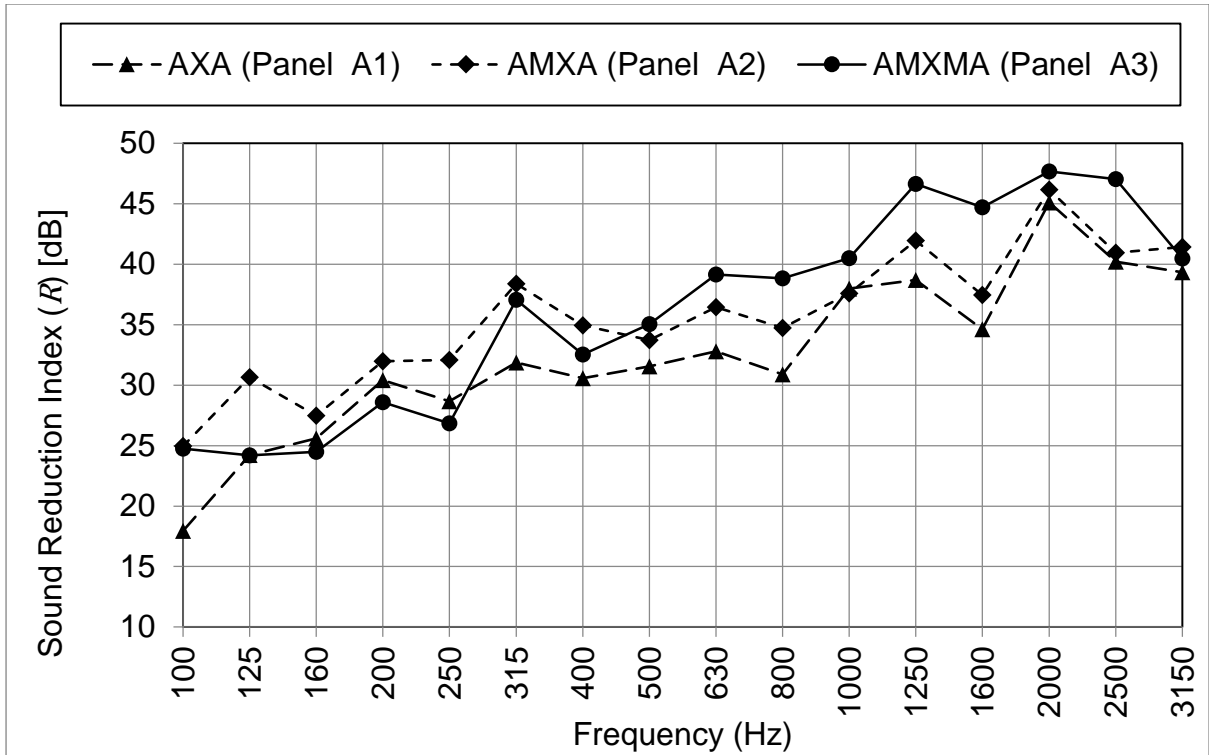


**Figure 8.** Measured sound reduction index (R) for different prototype CIPS

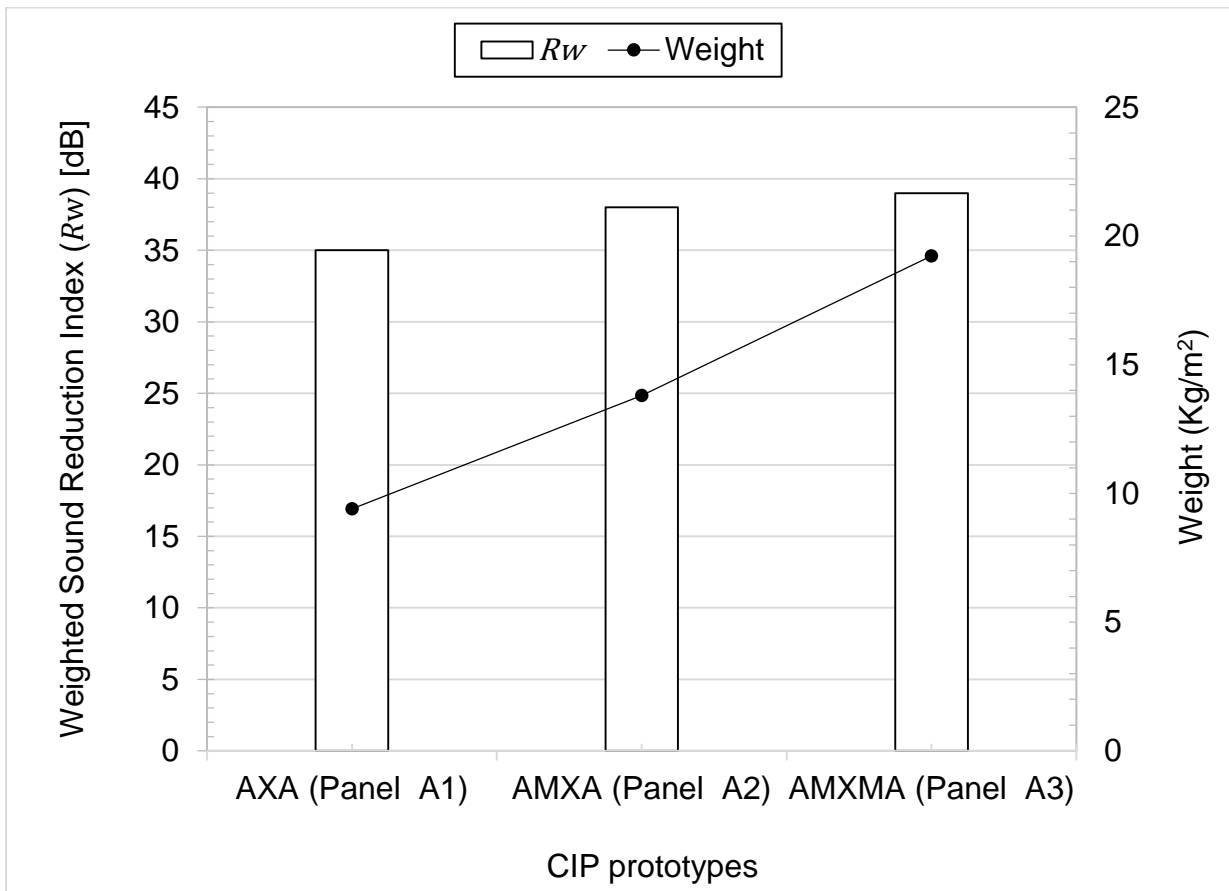


**Figure 9.** Comparison of weight and measured weighted sound reduction index ( $R_w$ )

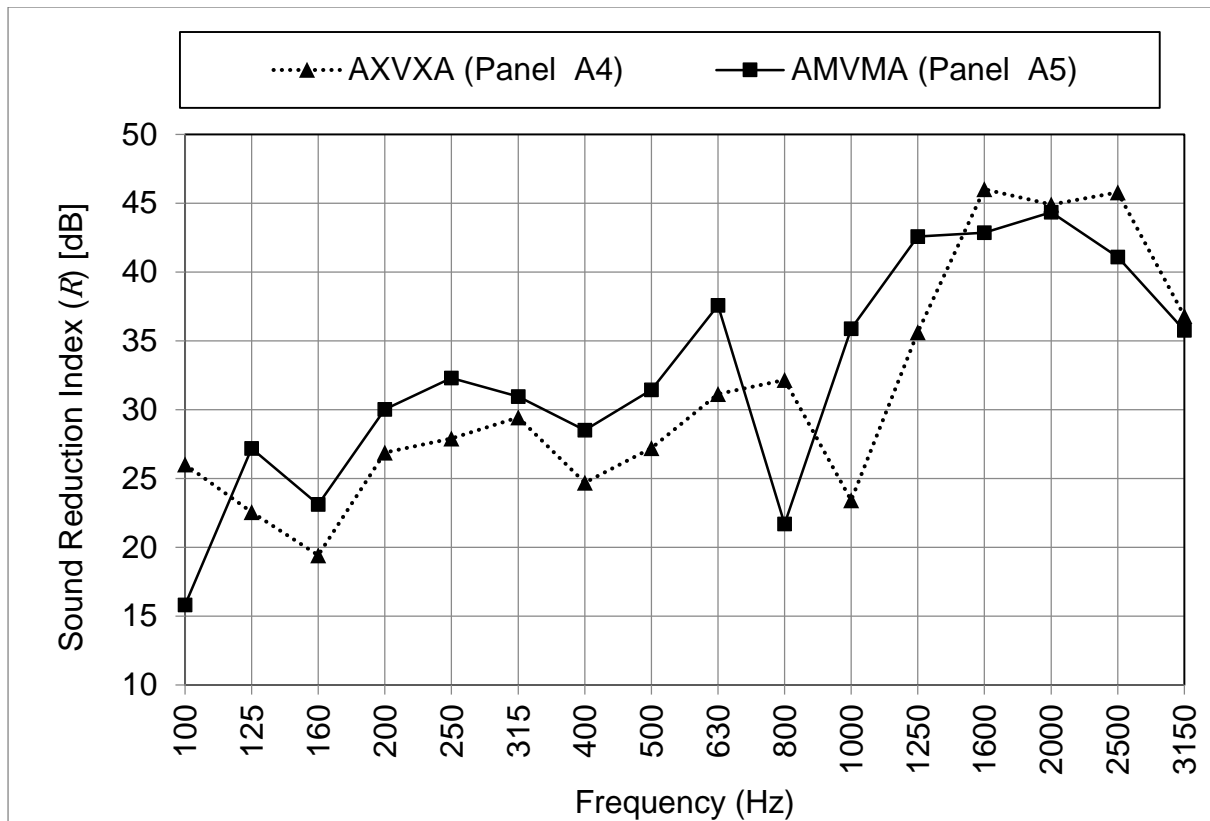


**Figure 10.** Effect of MLV layer on the sound reduction index ( $R$ ) of vacuum insulated CIPs

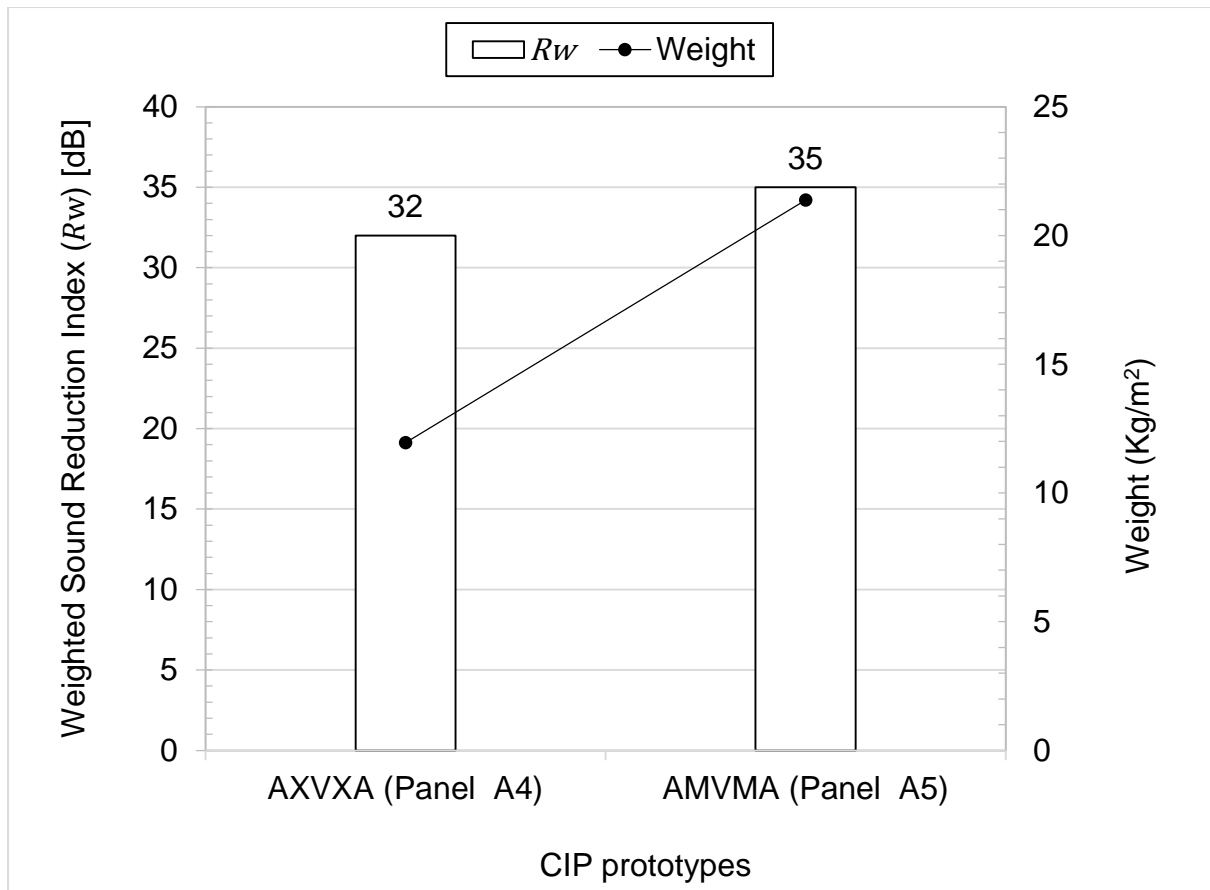


**Figure 11.** Measured weighted sound reduction ( $R_w$ ) and weight comparison of vacuum insulated CIPs